Bull. Chem. Soc. Jpn., 72, 1083—1091 (1999)

Thermodynamic Stabilities and Resonance Demand of Aromatic Radical Anions in the Gas Phase

Chul Huh, Chul Hyun Kang, Hai Whang Lee, Hirotaka Nakamura,† Masaaki Mishima,*,† Yuho Tsuno,† and Hiroshi Yamataka*,††

Department of Chemistry, Inha University, Inchon 402-751, Korea

†Institute for Fundamental Research of Organic Chemistry, Kyushu University, Hakozaki, Higashi-ku, Fukuoka 812-8581

††Institute of Scientific and Industrial Research, Osaka University, Mihogaoka 8-1, Ibaraki, Osaka 567-0047

(Received November 19, 1998)

The electron affinities (EAs) for a series of methyl benzoates, acetophenones, benzaldehydes, and benzophenones were determined by measuring the electron-transfer equilibria in the gas phase. The effect of substituents (X) in the benzene ring on the EAs of this series as well as the nitrobenzene and benzonitrile series were correlated in terms of the Yukawa–Tsuno equation,

$$\Delta \mathrm{EA} = \rho(\sigma^\circ + r^- \Delta\bar{\sigma}_\mathrm{R}^-). \qquad (1)$$

It has been shown that the r^- value, representing the degree of π-delocalization of the negative charge into the substituent (X) at position 4, increases linearly with decreasing EA of the unsubstituted member (X = H) of the respective series, i.e., 0.65 for nitrobenzene vs. 1.05 for benzaldehyde and 1.30 for benzonitrile. This tendency of the r^- value leads to the conclusion that the negative charge of a less-stable radical anion is more significantly distributed in the benzene ring than in a stable radical anion, like that of nitrobenzene. Ab initio MO calculations show that when the EA of a Y-substituted benzene decreases, the total negative charge on the substituent (Y) in the radical anion also decreases, and that the bond lengths (C2C3/C5C6) shorten. These features are consistent with the conclusion derived from the experimentally obtained r^- value.

The electron affinities (EAs) of organic compounds are of prime importance in understanding the electron-transfer processes in organic synthesis and biological reactions. In recent years, the relative electron affinities have been determined for a wide variety of organic compounds in the gas phase by measuring the equilibrium constants of electron-transfer reactions in a pulsed-ion cyclotron resonance (ICR) spectrometer[1,2] and a pulsed high-pressure ion source mass spectrometer (HPMS).[3—10] Much attention has been paid to substituent effects on the electron affinities of aromatic compounds ever since McIver's finding of a striking similarity of the substituent effect between the electron affinities of nitrobenzenes and the gas-phase acidities of phenols and anilines.[1] Kebarle and co-workers[3—9] analyzed the substituent effects on the EA of nitrobenzene, benzonitrile, pentafluorobenzene, and benzene, and found that those compounds with low EAs have a higher response to a change in the ring-substituent. They also observed a reversed-substituent effect between *p*-CHO and *p*-CN. In compounds with low EAs, such as the benzonitrile series, the *p*-CHO group gave a significantly higher EA than *p*-CN, while in the nitrobenzene series *p*-CN led to a higher EA than *p*-CHO.[6,7] This observation was interpreted in terms of an enhanced π-electron withdrawing effect relative to the field effect of substituents in compounds with low EAs.

Such a substituent behavior seems to be consistent with the concept of varying resonance demand introduced into the Yukawa–Tsuno (Y–T) equation (Eq. 1),[11,12]

$$P - P_\circ,\ \log K/K_\circ = \rho(\sigma^\circ + r^- \Delta\bar{\sigma}_\mathrm{R}^-), \qquad (1)$$

where σ° and $\Delta\bar{\sigma}_\mathrm{R}^-$ are the normal substituent and resonance substituent constant, respectively. The resonance demand parameter (r^-) represents the degree of π-delocalization of the negative charge into the aryl π-system. The Y–T analysis of the substituent effects on the gas-phase electron affinities should provide quantitative information about the nature of radical anions. In particular, we are interested in the variation of the r^- value as the thermodynamic stability of a radical anion changes, because in our previous study of the substituent effects on the gas-phase stability of benzylic carbocations, $\mathrm{ArC^+(R^1)R^2}$, the r^+ value, a measure of the π-delocalization of positive charge into the aryl π-system, was found to increase linearly with the decreasing stability of the unsubstituted member of the respective series.[13]

In order to elucidate the nature of the r^- value in the radical anion, it is necessary to analyze the substituent effects for a variety of aromatic compounds which cover a wide range of electron affinities. In this study, we therefore determined the EAs for a series of benzoyl compounds ($\mathrm{XC_6H_4Y}$: Y = CHO, COMe, CO_2Me, COC_6H_5) by applying the electron-transfer equilibrium method in the gas phase.

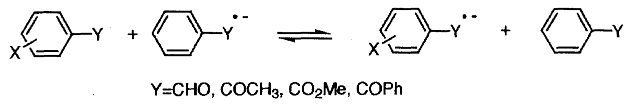

(2)

The EAs of several benzonitrile derivatives were also included in this study by way of a comparison. The EAs of the unsubstituted member of the respective aromatic compounds vary over 18 kcal mol^{-1} from nitrobenzene to methyl benzoate, giving a continuous spectrum of varying stability of the radical anions. We also carried out ab initio molecular-orbital calculations on these electron-transfer reactions in order to compare them with the experimental thermodynamic stabilities of radical anions and to obtain information about the geometric features of their related radical anions.

Results and Discussion

The equilibrium constants for the electron-transfer reaction,

$$A + B^{\bullet -} \rightleftarrows A^{\bullet -} + B, \qquad (3)$$

were measured on a pulsed ICR spectrometer built in our laboratory and an Extrel FTMS 2001 Fourier transform mass spectrometer. The free-energy changes of the respective electron-transfer equilibria in the gas phase are demonstrated in Fig. 1. Comparisons of the overlapping and successive steps on the ladder show an internal consistency of about 0.3 kcal mol^{-1}. This ladder provides a scale of relative EAs, because the entropy changes are generally small for such electron-transfer reactions in the gas phase.$^{1)}$ The absolute EA values can be obtained by calibrating the scale to the known EAs of anchor compounds. This scale includes many nitrobenzene derivatives, of which the EAs were independently determined in earlier studies by the McIver$^{1,2)}$ and Kebarle$^{3,8)}$ groups using a pulsed ICR and a pulsed HPMS, respectively. The ΔEAs of substituted nitrobenzenes relative to the unsubstituted derivative determined in this study agree well with those reported by Kebarle et al.,$^{3,8)}$

$$\Delta EA = 1.004\Delta EA_{(\mathrm{HPMS,\ Kebarle})} + 0.16 \quad (R = 0.999,\ n = 14). \quad (4)$$

The ΔEA values given by Kebarle's group can therefore be used for the present analysis. Since the EAs of methyl benzoate, acetophenone, and benzaldehyde could not be determined by the present electron-transfer equilibrium method, owing to poor electron affinity, we adopted the literature values$^{14-16)}$ obtained by the electron-capture detector (ECD) technique. These values are considered to be acceptable, because the EAs of 13.1 and 13.4 kcal mol^{-1} determined by the ECD for *p*- and *m*-chloroacetophenones,$^{17)}$ respectively, are in good agreement with the values determined in our present work. The ΔEAs of the respective series are listed in Table 1.

Substituent Effects on Electron Affinities. The ΔEAs of acetophenones, methylbenzoates, benzaldehydes, benzophenones, and benzonitriles are plotted against the corresponding values of nitrobenzenes (Figs. 2, 3, 4, 5, and 6). All of these plots reveal that there is no simple linear relationship which covers the whole range of substituents, which means that the substituent effect on EA varies significantly with the particular system. However, limited linear relationships are observed for *para* halogen and *meta* substituents, except for *m*-NO_2, *m*-CHO, and *m*-CO_2Me, as follows:

$$\Delta EA(\mathrm{acetophenone}) = 1.06\Delta EA(\mathrm{nitrobenzene}) - 0.40 \qquad (R = 0.997,\ n = 5), \quad (5)$$

$$\Delta EA(\mathrm{benzaldehyde}) = 1.10\Delta EA(\mathrm{nitrobenzene}) - 0.39 \qquad (R = 0.998,\ n = 7), \quad (6)$$

$$\Delta EA(\mathrm{methyl\ benzoate}) = 1.05\Delta EA(\mathrm{nitrobenzene}) + 0.15 \qquad (R = 0.995,\ n = 5), \quad (7)$$

$$\Delta EA(\mathrm{benzophenone}) = 0.797\Delta EA(\mathrm{nitrobenzene}) + 0.01 \qquad (R = 0.999,\ n = 6), \quad (8)$$

$$\Delta EA(\mathrm{benzonitrile}) = 1.18\Delta EA(\mathrm{nitrobenzene}) - 0.01 \qquad (R = 0.991,\ n = 5). \quad (9)$$

These excellent linear relationships indicate that the polar effects of these substituents consistently influence EA in all series, regardless of the different stabilities of their radical anions. On the other hand, *para* substituents having a large π-electron-withdrawing ability, such as *p*-NO_2 and *p*-CHO, distinctly deviate upward from this line. Figure 2 demonstrates that the magnitude of the deviation increases in the order $CF_3 < CN < CO_2Me < COMe$, $CHO < NO_2$. This order seems to be related to the π-electron accepting ability of the substituent. The same tendency in the effect of π-acceptors is observed for the other series, as shown in Figs. 3, 4, 5, and 6. Accordingly, the enhanced effects of *para* π-acceptors observed in compounds with low EAs are attributed to the increased resonance effects of these substituents compared to those in nitrobenzene.

The behavior of the *para* π-acceptors is consistent with the basic concept of the varying resonance demand introduced into the Yukawa–Tsuno equation (Eq. 1).$^{11,12)}$ Prior to the Y–T analysis of the substituent effects, it should be noted that *m*-NO_2, *m*-CHO, and *m*-CO_2Me deviate significantly upward from the linear relationship given by the other *meta*-substituents previously mentioned (Fig. 3). Similar enhanced effects of *meta* substituents are commonly observed in compounds with low EAs. The behavior of these *meta* substituents seems to exceed the perturbation treated by the substituent-effect analysis in the X,Y-disubstituted benzene system. This is not surprising, because the introduction of NO_2 at position 3 in the radical anion of compounds with low EAs must cause a large shift of the charge density to NO_2 owing to the higher EA of NO_2 compared to that of the fixed substituent (Y). The deviations observed for *m*-CHO and *m*-CO_2Me may also be similarly interpreted.

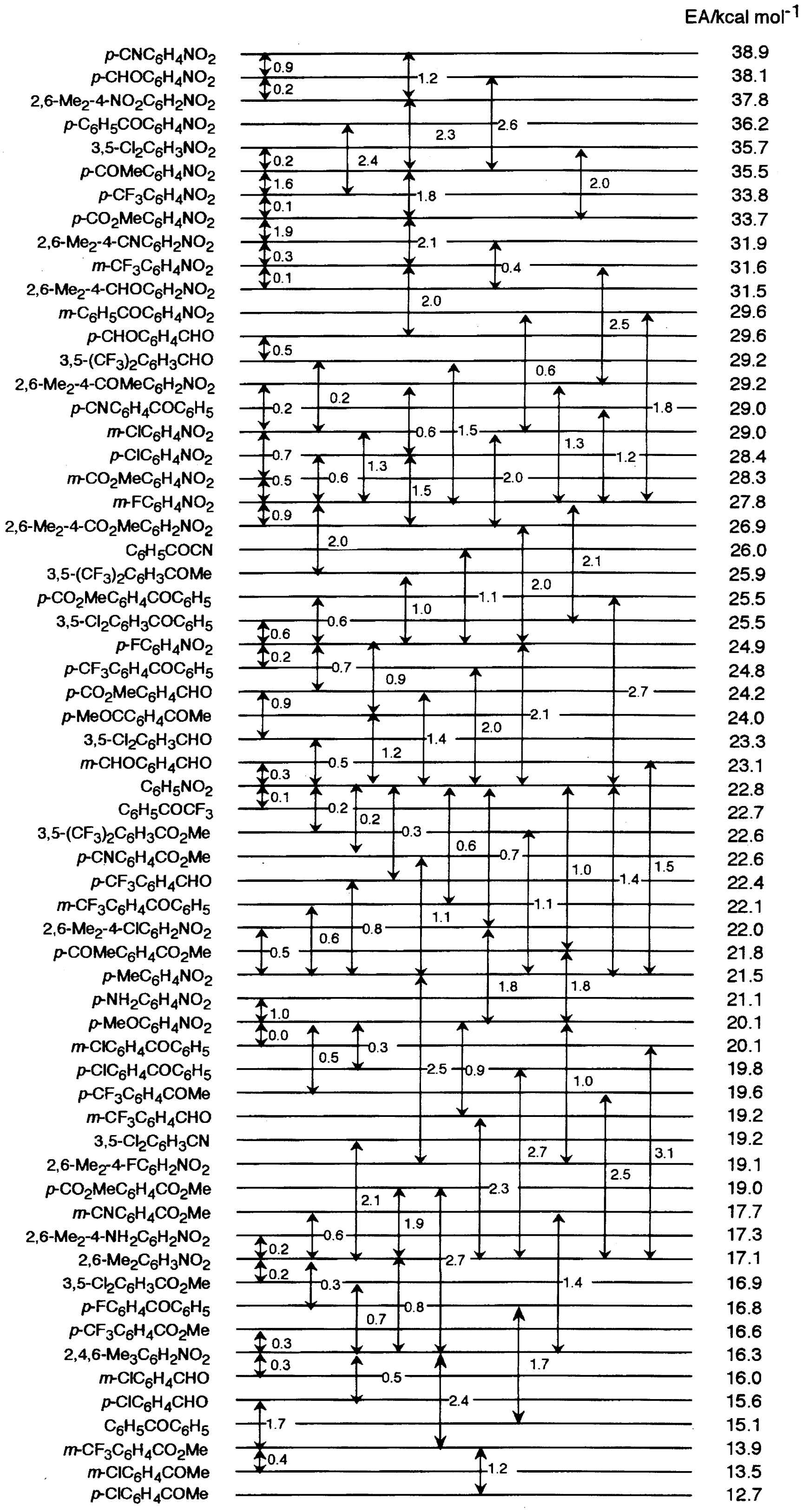

Fig. 1. Free energy changes for electron transfer reactions measured at 343 K. A scale of electron affinity is anchored by nitrobenzene (EA = 22.8 kcal mol^{-1}).[8)]

If these *meta* substituents are excluded, the ΔEAs of the aromatic compounds can be successfully correlated in terms of the Y–T equation (Eq. 1) by using a standard set of substituent constant values, σ° and $\Delta\bar{\sigma}_R^-$, for most of the substituents,[12)] although a new set of substituent constant values may be necessary for analyzing the substituent effects

Table 1. Relative Electron Affinities[a] of Benzene Derivatives and Substituent Constants

	Y						Substituent constants[b]	
Subst. (X)	CO_2Me	COMe	CHO	COPh	CN[c]	NO_2[d]	σ°	$\Delta\bar{\sigma}_R^-$
p-NO_2	29.4	27.8	28.1	21.2	33.6	21.5	0.810	0.61[f]
p-CN	18.4	17.3	18.2	14.0	20.3	15.9	0.653	0.30
p-CHO	20.3	—	19.8	—	22.6	14.9	0.510	0.47
p-CF_3	12.6	12.3	12.7	9.8	13.1	11.0	0.505	0.15[f]
p-COMe	17.9	16.7	—	—	19.5[e]	12.7	0.491	0.36
p-CO_2Me	15.0	14.4	14.6	10.8	17.1[e]	10.8	0.460	0.30
m-NO_2	24.1	21.9	21.8	14.5	29.3	14.1	0.71	0
m-CN	13.5	—	13.3	—	15.5	12.0	0.607	0
m-CHO	—	—	13.4	—	17.7	8.9	0.415	0
m-CO_2Me	—	—	—	—	12.2[e]	5.5	0.36	0
m-CF_3	9.8	9.3	9.8	7.2	10.0	8.8	0.493	0
3,5-$(CF_3)_2$	18.6	18.4	19.4	—	20.8	17.4	0.986	0
3,5-Cl_2	12.7	—	13.8	10.5	13.7[e]	12.4	0.720	0
m-Cl	—	5.9	6.4	5.1	—	6.0	0.373	0
p-Cl	—	5.1	6.2	4.5	—	5.4	0.281	0
p-F	—	—	—	1.7	—	2.2	0.212	0
H[g]	0.0	0.0	0.0	0.0	0.0	0.0	0.0	0
	(4.2)[h]	(7.7)[i]	(9.9)[j]	(15.3)[k]	(5.5)[j]	(22.8)[d]		

a) $-\delta\Delta G^\circ$ at 343 K in kcal mol^{-1}, 1 cal = 4.184 J. b) Ref. 12. c) Ref. 7. d) Ref. 8. e) Determined in this study. f) Standard $\Delta\bar{\sigma}_R^-$ values for NO_2 and CF_3 are 0.455 and 0.196, respectively, Ref. 12. g) Values in parentheses denote absolute EAs. h) Ref. 14. i) Ref. 15. j) Ref. 16. k) Ref. 8.

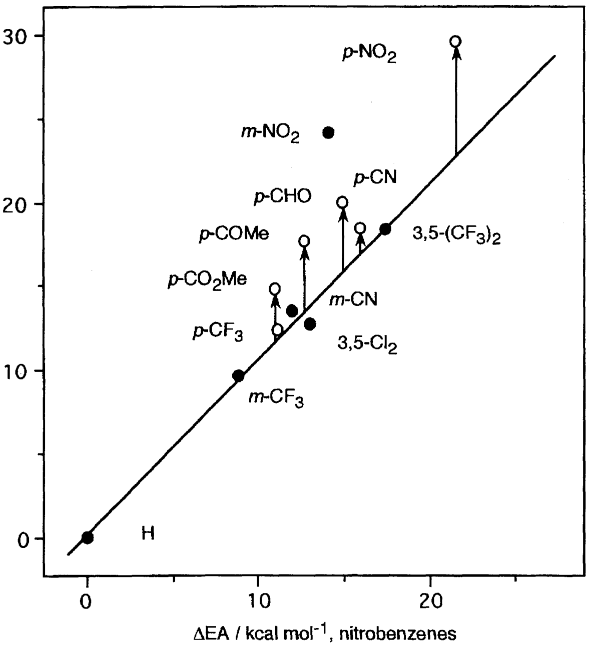

Fig. 2. Plot of ΔEA for methyl benzoates vs. nitrobenzenes. Closed circles; *meta* substituents, open circles; *para* π-acceptors.

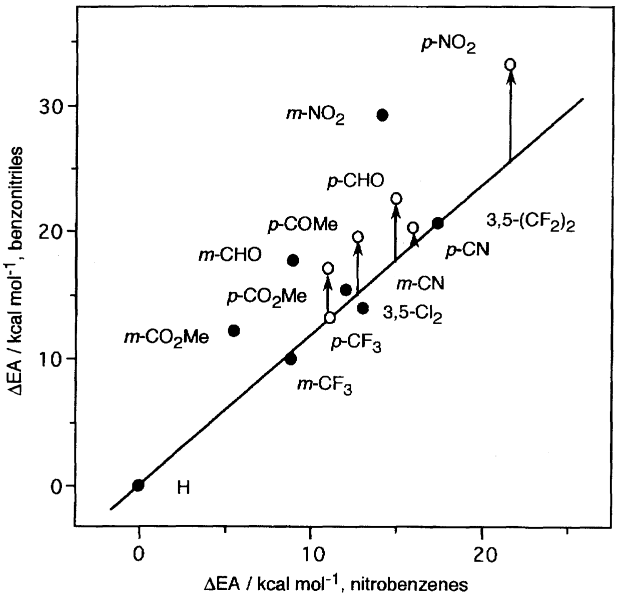

Fig. 3. Plot of ΔEA for benzonitriles vs. nitrobenzenes. Closed circles; *meta* substituents, open circles; *para* π-acceptors.

of odd-electron anion systems. The standard substituent constants based on an even-electron anion systems, like the acidities of phenols in solution, seem to apply to the present systems as a first approximation. This suggests that the thermodynamic stabilities of radical anions mainly reflect their properties as anions rather than radicals. An exception is seen for the *p*-NO_2 group, which consistently has a larger electron-withdrawing effect in all series compared to that expected by the standard substituent constant values ($\sigma^\circ = 0.810$ and $\Delta\bar{\sigma}_R^- = 0.455$). Iterative analyses of the substituent effects give an average value of 0.61 for $\Delta\bar{\sigma}_R^-$ of the *p*-NO_2 group. Such an enhanced resonance effect may be characteristic of the radical anion. In addition, it is found that a small modification of the $\Delta\bar{\sigma}_R^-$ value for *p*-CF_3 may be necessary in these substituent effects. The correlation results obtained by using modified substituent constants are given in Table 2.

The ρ values are almost constant at 19.2±1.0, indicating

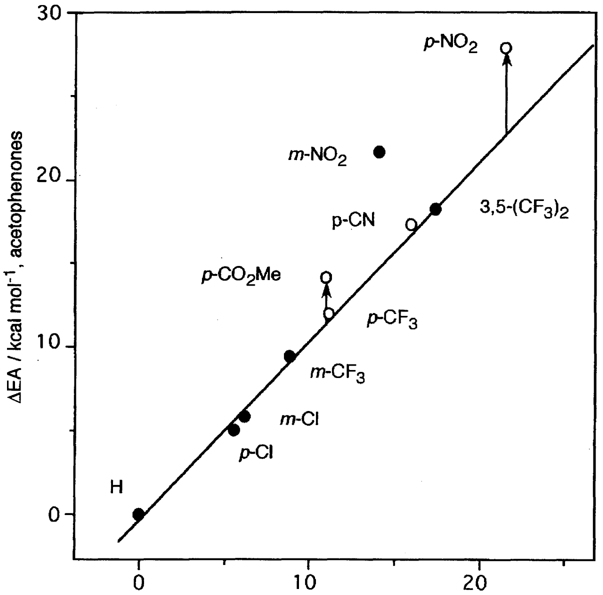

Fig. 4. Plot of ΔEA for acetophenones vs. nitrobenzenes. Closed circles; *meta* substituents and *para* π-donor, open circles; *para* π-acceptors.

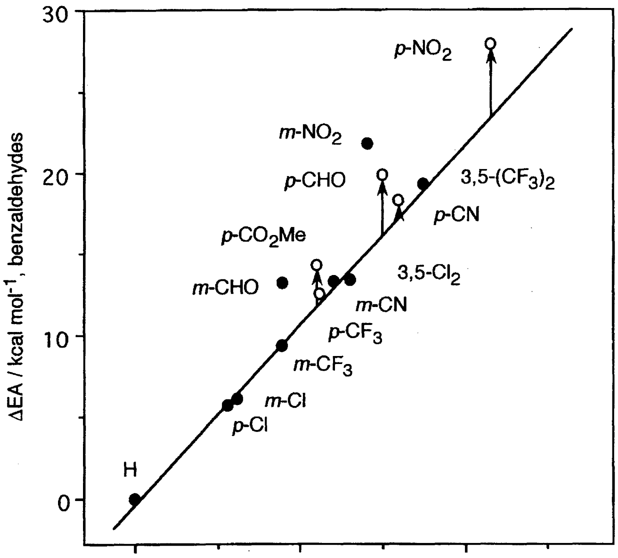

Fig. 5. Plot of ΔEA for benzaldehydes vs. nitrobenzenes. Closed circles; *meta* substituents and *para* π-donor, open circles; *para* π-acceptors.

that the magnitude of the ρ value is independent of the stability of the parent radical anion. The ρ value of 15.0 for the benzophenone series is exceptionally small. Although the reason for this is unclear at the present stage, it may be due to the varying effect of the fixed phenyl group, depending on the effect of the substituted phenyl group. That is, since one phenyl group has a strong electron-withdrawing substituent, the effect of the fixed phenyl may be reduced. This would lower the response of EA to changing substituents, resulting in a small ρ value. The most important feature of

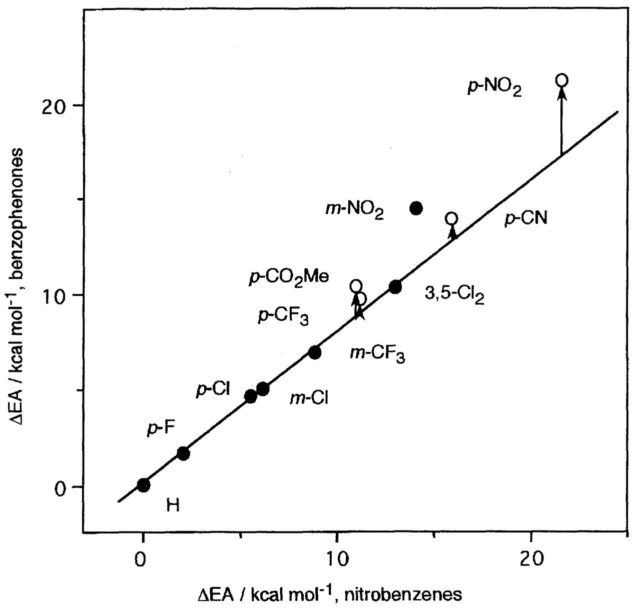

Fig. 6. Plot of ΔEA for benzophenones vs. nitrobenzenes. Closed circles; *meta* substituents and *para* π-donors, open circles; *para* π-acceptors.

Table 2. Correlation Results in Terms of the Yukawa–Tsuno Equation, $\Delta\mathrm{EA} = \rho(\sigma^{\circ} + r^{-}\Delta\bar{\sigma}_{\mathrm{R}}^{-})$

Series	ρ	r^-	±SD[a]	R[b]
Nitrobenzene	18.3	0.65	0.60	0.995
Benzophenone	15.0	1.00	0.61	0.996
Benzaldehyde	19.5	1.05	0.48	0.998
Acetophenone	18.7	1.11	0.53	0.998
Benzonitrile	20.9	1.30	0.74	0.997
Methyl benzoate	18.6	1.25	0.52	0.998

a) Standard deviations. b) Correlation coefficients.

Table 2 is that the r^- value varies significantly from 0.65 for nitrobenzene to 1.30 for benzonitrile, as expected from a graphical analysis. The significantly enhanced resonance demand in a less-stable radical anion supports Kebarle's interpretation for the reversed substituent effect between *p*-CHO and *p*-CN characteristic of the compounds with low EAs.[6,7] That is, the enhanced resonance effect in compounds with low EAs results in a larger EA of the *p*-CHO over *p*-CN derivative, because the π-electron withdrawing effect of CHO ($\Delta\bar{\sigma}_{\mathrm{R}}^{-} = 0.47$) is greater than that of CN (0.30), while *p*-CN provides a higher EA than *p*-CHO in nitrobenzene. A similar reversed-substituent effect is observed for the pair of *p*-$\mathrm{CO_2Me}$ and *p*-$\mathrm{CF_3}$ substituents. The former gave a higher EA than the latter in compounds with low EAs while in the nitrobenzene series the order was reversed. This result can be similarly interpreted, because *p*-$\mathrm{CO_2Me}$ ($\Delta\bar{\sigma}_{\mathrm{R}}^{-} = 0.30$) has a larger resonance effect than does *p*-$\mathrm{CF_3}$ (0.15).

The order of the increasing r^- value is consistent with that of the decrease in the EA of the unsubstituted member of the respective series. In fact, a plot of the r^- values against the EA's gives a good linear relationship (Fig. 7). A least-squares analysis of this data gives the following correlation

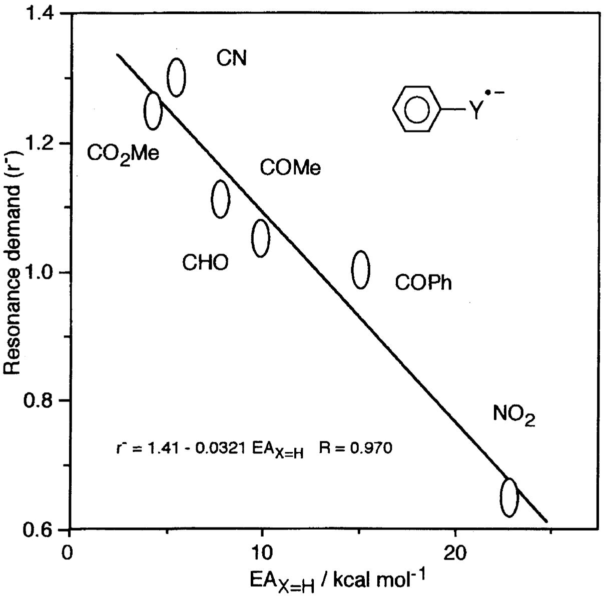

Fig. 7. Plot of resonance demand (r^-) against EA of the unsubstituted member of respective series.

with a correlation coefficient of 0.97:

$$r^- = -0.032\mathrm{EA}_{\mathrm{X=H}} + 1.41. \tag{10}$$

A similar linear relationship was previously found for substituent effects on the stabilities of benzylic carbocations, $\mathrm{ArC^+(R^1)R^2}$. The resonance demand (r^+) increases linearly with the decreasing stability of the unsubstituted member of each series,[13c)]

$$r^+ = -0.026\Delta\Delta G^\circ_{\mathrm{X=H}} + 1.00, \tag{11}$$

where $\Delta\Delta G^\circ_{\mathrm{X=H}}$ is the stability of the unsubstituted member of the respective benzylic carbocations relative to the α-cumyl cation (1-methyl-1-phenylethyl cation). Interestingly, the coefficient of the $\mathrm{EA}_{\mathrm{X=H}}$ term in Eq. 10 is close to that of $\Delta\Delta G^\circ_{\mathrm{X=H}}$ in Eq. 11, indicating that both r^+ and r^- have a similar response to the thermodynamic stability of the ions. These facts support our previous conclusion that the origin of the varying resonance demand is the change in the intrinsic stability of the parent ion.[13)]

Theoretical Calculations. Since the observed gas-phase EAs are free from solvent effects, the theoretical values given by ab initio molecular-orbital calculations should be directly comparable with the experimental values. The geometries of radical anions and the corresponding neutral molecules were optimized for 20 representative derivatives at the ROHF and HF level of theory, respectively, with the 6-31+G* basis set. Single-point calculations at the MP2/6-31+G* level of theory[18)] were carried out on the obtained geometries. The energy changes for the isodesmic reaction (12) are given in Table 3.

$$\mathrm{XC_6H_4Y + C_6H_5NO_2^{\bullet-} \rightleftarrows XC_6H_4Y^{\bullet-} + C_6H_5NO_2} \tag{12}$$

These quantities correspond to the relative electron affinities, which can be determined experimentally. In Fig. 8 are plotted the calculated ΔEAs against the observed ones. A good linear correlation,

$$\Delta\mathrm{EA_{obsd}} = 0.87\Delta\mathrm{EA_{calcd}} + 1.2 \ (R = 0.985), \tag{13}$$

is obtained by a least-squares method. This indicates that ab initio MO calculations at the present level of theory can satisfactorily reproduce the ΔEAs of these compounds. The energy of the LUMO of the neutral molecule are also obtained by these calculations. They are summarized in Table 4. It

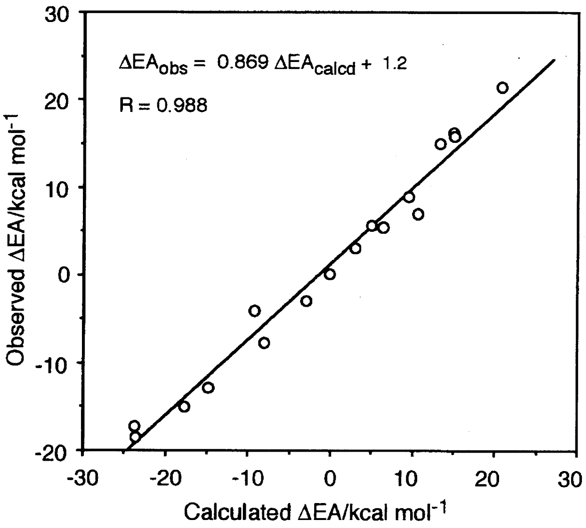

Fig. 8. Comparison between calculated and observed ΔEAs.

Table 3. Calculated Relative Electron Affinities[a)] of Aromatic Compounds at MP2/6-31+G*//HF/6-31+G*

Compounds	ΔEA/ kcal mol^{-1}	Compounds	ΔEA/ kcal mol^{-1}
$\mathrm{C_6H_5NO_2}$	0.00	*m*-$\mathrm{CF_3C_6H_4NO_2}$	9.60
$\mathrm{C_6H_5COPh}$	−8.08	*m*-$\mathrm{CO_2MeC_6H_4NO_2}$	5.04
$\mathrm{C_6H_5CHO}$	−14.77	*m*-$\mathrm{CHOC_6H_4NO_2}$	9.47
$\mathrm{C_6H_5COMe}$	−17.61	*p*-$\mathrm{CHOC_6H_4CHO}$	10.64
$\mathrm{C_6H_5CN}$	−23.63	*p*-$\mathrm{CNC_6H_4CHO}$	6.48
$\mathrm{C_6H_5CO_2Me}$	−23.69	*m*-$\mathrm{CF_3C_6H_4CHO}$	−2.89
p-$\mathrm{NO_2C_6H_4NO_2}$	20.77	*m*-$\mathrm{CF_3C_6H_4CN}$	−1.88
p-$\mathrm{CNC_6H_4NO_2}$	14.97	*p*-$\mathrm{CNC_6H_4CN}$	−9.35
p-$\mathrm{CHOC_6H_4NO_2}$	13.25	*p*-$\mathrm{CHOC_6H_4CN}$	3.09
m-$\mathrm{NO_2C_6H_4NO_2}$	13.93	*m*-$\mathrm{CHOC_6H_4CHO}$	6.48

a) Energy changes for the isodesmic reaction (12).

Table 4. Calculated Orbital Energies[a)] of LUMO for Neutral Molecules at MP2/6-31+G*//HF/6-31+G*

Compounds	LUMO	Compounds	LUMO
$C_6H_5NO_2$	25.4	m-$CO_2MeC_6H_4NO_2$	21.8
C_6H_5CHO	39.2	m-$CHOC_6H_4NO_2$	14.6
C_6H_5CN	39.2	m-$NO_2C_6H_4NO_2$	7.7
C_6H_5COPh	39.8	m-$CF_3C_6H_4CHO$	30.0
$C_6H_5CO_2Me$	43.9	m-$CHOC_6H_4CHO$	24.2
C_6H_5COMe	41.5	p-$CHOC_6H_4CHO$	18.4
p-$NO_2C_6H_4NO_2$	−2.3	m-$CF_3C_6H_4CN$	32.3
p-$CHOC_6H_4NO_2$	6.9	p-CNC_6H_4CN	18.4
m-$CF_3C_6H_4NO_2$	16.1	p-$CHOC_6H_4CN$	18.4
p-$CNC_6H_4NO_2$	6.9		

a) In kcal mol^{-1}.

is interesting to compare the observed EAs with the energy of the LUMO of the neutral molecule, because an added electron to a neutral molecule enters the LUMO. Figure 9 shows that there is a good linear relationship between the energies of the LUMO and the observed EAs,

$$E_{\mathrm{LUMO}} = -1.09\mathrm{EA}_{\mathrm{obsd}} + 49.9 \quad (R = 0.983), \qquad (14)$$

i.e., the lower LUMO gives the higher electron affinity, indicating that the electron affinity strongly reflects the character of the LUMO of neutral molecule, as expected.

The selected geometric parameters of the radical anions and neutral molecules are given in Table 5. The charge densities on atoms and/or groups, derived from a natural-population analysis (NPA) of the MP2/6-31+G* orbitals, calculated for the optimized geometry at ROHF/6-31+G* level, are summarized in Table 6. For most radical anions, the C1C2/C1C6 and C3C4/C4C5 bonds lengthen, whereas the C2C3/C5C6 bonds shortens compared to those for the corresponding neutral molecules. According to the Jahn–Teller theorem,[19)] the benzene radical anion distorts and the degenerate $^2E_{2u}$ electronic state splits into ^2A_u and $^2B_{1u}$ components (Scheme 1).[20)] The calculated geometrical features

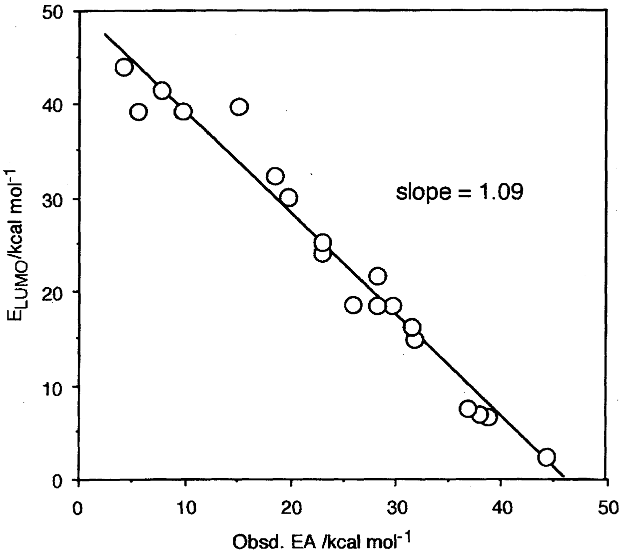

Fig. 9. Plot of E_{LUMO} of neutral molecules against $\Delta EA_{\mathrm{obsd}}$.

Table 6. Calculated Charge Density[a)] of Radical Anions of Monosubstituted Benzenes

Radical anion	Y[b)]	C1	(C2+C6)/2[c)]	(C3+C5)/2[c)]	C4
$C_6H_5NO_2$	−1.029	0.108	0.028	−0.038	−0.059
C_6H_5COPh	−0.672	−0.076	−0.019	−0.023	−0.111
C_6H_5CHO	−0.476	−0.263	−0.010	−0.065	−0.111
C_6H_5COMe	−0.474	−0.263	−0.010	−0.065	−0.114
C_6H_5CN	−0.236	−0.408	−0.022	−0.077	−0.159
$C_6H_5CO_2Me$	−0.330	−0.239	−0.032	−0.038	−0.223

a) Derived from natural population analysis (NPA) of the MP2/6-31+G* orbitals calculated for the optimized geometry of radical anions at HF/6-31+G*. b) Summed charge density on the substituent Y. c) Average of two positions.

Table 5. Selected Geometric Parameters[a)] of Radical Anions and Neutral Molecules

	Bond length (Å)[b)]			Angle
Compound	C1C2/C1C6	C2C3/C5C6	C3C4/C4C5	∠C2C1C6[c)]
Radical anions				
$C_6H_5NO_2$	1.401	1.384	1.388	119.0
C_6H_5COPh	1.412	1.384	1.392	116.2
C_6H_5CHO	1.431	1.374	1.404	116.3
C_6H_5COMe	1.434	1.375	1.403	115.9
$C_6H_5CO_2Me$	1.437	1.370	1.410	116.6
C_6H_5CN	1.439	1.366	1.417	117.2
Neutral molecules				
$C_6H_5NO_2$	1.384	1.385	1.388	122.4
C_6H_5COPh	1.388	1.382	1.385	119.4
C_6H_5CHO	1.392	1.385	1.389	119.9
C_6H_5COMe	1.393	1.386	1.388	119.0
$C_6H_5CO_2Me$	1.391	1.386	1.389	119.9
C_6H_5CN	1.392	1.385	1.388	120.5

Numbering of atoms given in Scheme 1. a) Optimized at ROHF/6-31+G* and HF/6-31+G* for radical anions and neutral molecules, respectively. b) Average of two bond lengths. c) In degrees.

Scheme 1.

suggest that the $^2B_{1u}$ structure is favored for these radical anions. An exception was the nitrobenzene radical anion. The C3C4/C4C5 and C2C3/C5C6 bond lengths are nearly identical, also lying close to those of nitrobenzene. The geometric features of the nitrobenzene radical anion indicate that the $^2B_{1u}$ structure is less important. This may be due to the high electron affinity of the nitro group. In fact, the calculated charge density reveals that the negative charge is mostly located on the nitro group, whereas in compounds with low EAs, such as methyl benzoate and benzonitrile, the negative charge is mainly distributed in the benzene ring. This result is consistent with the fact that the substituent effect for the EAs of the 2,6-dimethyl-4-substituted nitrobenzenes agrees with that for the untwisted nitrobenenzene series, although the π-interaction of the nitro group with the benzene ring is markedly reduced in the 2,6-dimethyl nitrobenzene system, owing to a twisting out of the benzene plane.[21]

Furthermore, it was found that when the electron affinity of Y-substituted benzene decreases the charge density on Y also decreases and the C2C3/C5C6 bonds shorten, thereby favoring the $^2B_{1u}$ structure. In addition, the charges on Y of nitrobenzene, benzaldehyde, and benzonitrile were found to diminish with the increasing electron-withdrawing ability of the X-substituent. Thus, the thermodynamic properties of radical anions are closely related to the extent of the distribution of the negative charge in the anion.

It is worth examining the substituent effects on the calculated EAs in connection with the experimental observation that the resonance effect of the π-acceptor involved in the susbstituent effect changes with the variation of the Y-substituent. The calculated ΔEAs of benzonitrile are plotted against those of the nitrobenzene series (Fig. 10). There is no simple linear relationship between the two substituent effects. However, the plot resembles that for the experimental values (Fig. 3). In other words, if a straight line is drawn through the H and *m*-CF_3, large upward deviations from this line are found for the strong *para* π-acceptors, *p*-NO_2 and *p*-CHO, and only a small deviation is seen for the weak π-acceptor, *p*-CN. Therefore, the strong π-acceptors stabilize the radical anion of benzonitrile more effectively than nitrobenzene. Thus, the theoretical calculation reproduces varying r^- values with the system; namely, increasing r^- values appear along with decreasing electron affinity of the unsubstituted member of the respective series. This result encourages us to compare the r^- values with the theoretical parameters of the radical anions. It is found that the r^- values are linearly correlated with the negative charges on Y (Fig. 11). In addition, the C2C3 and C5C6 bonds shorten and the C1C2/C1C5 and C3C4/C4C5 bonds lengthen when the r^- value increases. These results suggest that the enhanced π-interaction between the *para* π-acceptor and the large negative charge in the benzene ring is responsible for the increase in the r^- value. Consequently, in the less-stable radical anion the negative charge is essentially distributed throughout the whole molecule by a resonance interaction between the π-acceptor substituents and the benzene ring.

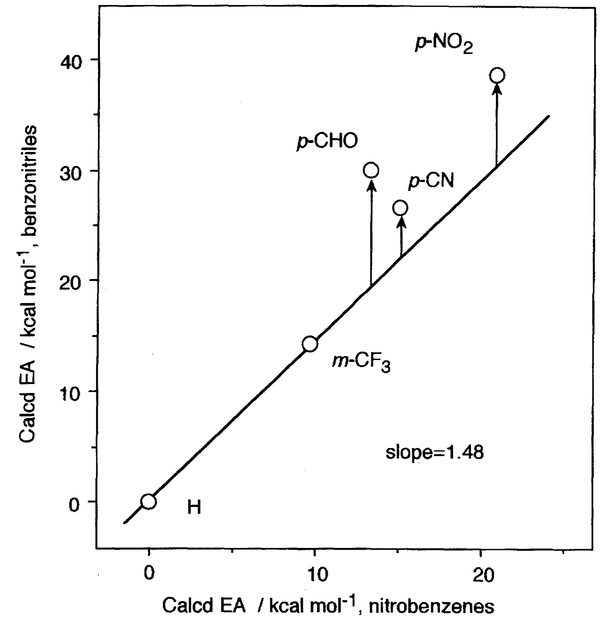

Fig. 10. Plot of calculated ΔEA, benzonitriles vs. nitrobenzenes.

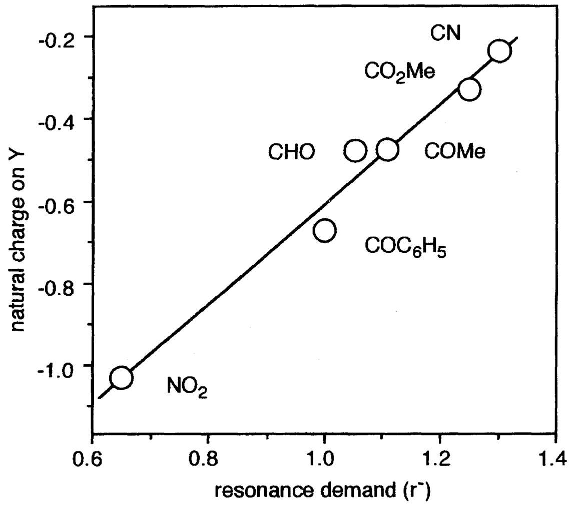

Fig. 11. Linear relationship between the resonance demand (r^-) and the charge density on Y of Y-substituted benzenes.

Conclusions

The substituent effects on the stabilities of aromatic radical anions have been successfully analyzed using the Yukawa–Tsuno equation in the same manner as that of an even-electron anion. It has been shown that the r^- value, a measure of the contribution of the resonance effect by *para* π-acceptors, increases linearly with decreasing stability of the unsubstituted member of the respective radical anions. The behavior in the substituent effect could be reproduced by ab initio MO calculations. The variation in the resonance demand by the system is reasonably related to the theoretical parameters, such as the charge densities and bond lengths of the radical anions.

Experimental

Compounds. Most of the compounds used in this study were obtained from commercial sources; the others were available from previous studies.[22)]

ICR Measurements. Equilibrium-constant measurements for the electron-transfer reactions were performed on a pulsed ICR spectrometer built in our laboratory and an Extrel FTMS 2001 Fourier-transform mass spectrometer. The experimental techniques employed in this study were the same as those described by McIver et al.[2)] Only significant changes and/or additional procedures will be given here. All measurements were performed at 70 °C under a 1.3 T or 3 T uniform magnetic-field strength. The pressures of neutral reactants were measured by means of a Bayard–Alpert type ionization gauge with appropriate correction factors being applied to correct the gauge readings for the different ionization cross-sections of different compounds.[23)] In order to minimize the formation of dimeric ions, the overall pressures of the reactants were maintained at between 10^{-7} to 10^{-8} Torr (1 Torr = 133.322 Pa) by controlled rates through leak valves from a parallel inlet manifold into the vacuum chamber. Each sample was subjected to several freeze-pump-thaw cycles on the ICR inlet vacuum system to remove any entrapped impurities. The electron-transfer reactions were initiated by a 5 ms pulse of a low-energy electron beam (1—2 eV) through the ICR cell.

$$\mathrm{A} + \mathrm{e}^- \rightarrow \mathrm{A}^{\bullet-} \tag{15}$$

$$\mathrm{B} + \mathrm{e}^- \rightarrow \mathrm{B}^{\bullet-} \tag{16}$$

$$\mathrm{A} + \mathrm{B}^{\bullet-} \rightleftarrows \mathrm{A}^{\bullet-} + \mathrm{B} \tag{17}$$

$$K = [\mathrm{A}^{\bullet-}]\ [\mathrm{B}]/[\mathrm{B}^{\bullet-}]\ [\mathrm{A}] \tag{18}$$

$$\Delta G^\circ = -RT\ln K \tag{19}$$

After a reaction period of 1 to 5 s, depending on the reactant, equilibrium was attained, and the relative abundance of A^- and B^- was measured based on the signal intensities of the ICR spectra. The equilibrium constant (K) and free energy change (ΔG°) were calculated from the relative abundance of two negative ions and the partial pressures of the neutral molecules. The average uncertainty of ΔG° was estimated to be less than ± 0.2 kcal mol^{-1} for most cases. Each experiment was performed at several ratios of the partial pressures and at different overall pressures.

Ab initio Calculations. Ab initio MO calculations were carried out for representative radical anions and the corresponding neutral derivatives. All calculations were performed using the Gaussian 94 program.[24)] The Hartree–Fock calculation with 6-31+G* basis set was applied to find the stationary point on the potential-energy surface. To improve the calculated energies, single-point MP2 calculations were also carried out at the 6-31+G* basis set using the frozen-core approximation.

The authors gratefully acknowledge support for this research by a Grant-in-Aid for Scientific Research from Ministry of Education, Science, Sports and Culture.

References

1) E. K. Fukuda and R. T. McIver, Jr., *J. Phys. Chem.*, **87**, 2993 (1983).

2) E. K. Fukuda and R. T. McIver, Jr., *J. Am. Chem. Soc.*, **107**, 2291 (1985).

3) E. P. Grimsrud, G. Caldwell, S. Chowdhury, and P. Kebarle, *J. Am. Chem. Soc.*, **107**, 4627 (1985).

4) P. Kebarle and S. Chowdhury, *Chem. Rev.*, **87**, 513 (1987).

5) S. Chowdhury, E. P. Grimsrud, T. Heinis, and P. Kebarle, *J. Am. Chem. Soc.*, **108**, 3630 (1986).

6) S. Chowdhury, T. Heinis, and P. Kebarle, *J. Am. Chem. Soc.*, **108**, 4662 (1986).

7) S. Chowdhury and P. Kebarle, *J. Am. Chem. Soc.*, **108**, 5453 (1986).

8) S. Chowdhury, S. C. Kishi, G. W. Dillow, and P. Kebarle, *Can. J. Chem.*, **67**, 603 (1989).

9) G. W. Dillow and P. Kebarle, *J. Am. Chem. Soc.*, **111**, 5592 (1989).

10) L. Crocker, T. Wang, and P. Kebarle, *J. Am. Chem. Soc.*, **115**, 7818 (1993).

11) Y. Yukawa, Y. Tsuno, and M. Sawada, *Bull. Chem. Soc. Jpn.*, **39**, 2274 (1966).

12) Y. Tsuno, M. Fujio, Y. Takai, and Y. Yukawa, *Bull. Chem. Soc. Jpn.*, **45**, 1519 (1972).

13) a) M. Mishima, K. Arima, H. Inoue, S. Usui, M. Fujio, and Y. Tsuno, *Bull. Chem. Soc. Jpn.*, **68**, 3199 (1995); b) M. Mishima, H. Inoue, S. Itai, M Fujio, and Y. Tsuno, *Bull. Chem. Soc. Jpn.*, **69**, 3273 (1996); c) M. Mishima, H. Inoue, M Fujio, and Y. Tsuno, *Bull. Chem. Soc. Jpn.*, **70**, 1163 (1997).

14) W. F. Kuhn, R. J. Levons, and A. C. Lilly, Jr., *J. Chem. Phys.*, **49**, 5550 (1968).

15) W. E. Wentworth and E. Chen, *J. Phys. Chem.*, **71**, 1929 (1967).

16) W. E. Wentworth, L. W. Kao, and R. S. Becker, *J. Phys. Chem.*, **79**, 1161 (1975).

17) J. C. Steelhammer and W. E. Wentworth, *J. Chem. Phys.*, **51**, 1802 (1969).

18) MP2: C. Møller and M. S. Plesset, *Phys. Rev.*, **46**, 618 (1934). 6-31G*: P. C. Hariharan and J. A. Pople, *Theor. Chim. Acta*, **28**, 213 (1973); M. M. Francl, W. L. Pietro, W. L. Hehre, J. S. Binkley, M. S. Gordon, D. J. DeFrees, and J. A. Pople, *J. Chem. Phys.*, **77**, 3654 (1982).

19) H. A. Jahn and E. Teller, *Proc. R. Soc. London, Ser. A*, **161**, 220 (1937); H. A. Jahn, *Proc. R. Soc. London, Ser. A*, **164**, 117 (1938).

20) A. L. Hinde, L. Radom, and D. Poppinger, *J. Am. Chem. Soc.*, **100**, 4681 (1978).

21) M. Mishima, C. H. Kang, M. Fujio, and Y. Tsuno, *Chem. Lett.*, **1993**, 889.

22) M. Mishima, Mustanir, M. Fujio, and Y. Tsuno, *Bull. Chem. Soc. Jpn.*, **69**, 2009 (1996).

23) J. E. Bartmess and R. M. Georgiadis, *Vacuum*, **33**, 149 (1983); K. J. Miller, *J. Am. Chem. Soc.*, **112**, 8533 (1990).

24) M. J. Frisch, G. W. Trucks, H. B. Schlegel, P. M. W. Gill, B. G. Johnson, M. A. Robb, J. R. Cheeseman, T. Keith, G. A. Petersson, J. A. Montgomery, K. Raghavachari, M. A. Al-Laham, V. G. Zakrzewski, J. V. Ortiz, J. B. Foresman, J. Cioslowski, B. B. Stefanov, A. Nanayakkara, M. Challacombe, C. Y. Peng, P. Y. Ayala, W.Chen, M. W. Wong, J. L. Andress, E. S. Replogle, R. Gomperts, R. L. Martin, D. J. Fox, J. S. Binkley, D. J. Defrees, J. Baker, J. P. Stewart, M. Head-Gordon, C. Gonzalez, and J. A. Pople, "GAUSSIAN 94, Revision C.2," Gaussian, Inc., Pittsburgh, PA (1995).